Including Anharmonicity in the Calculation of Rate Constants. 1. The HCN/HNC Isomerization Reaction†

Alan D. Isaacson*

Department of Chemistry and Biochemistry, Miami University, Oxford, Ohio 45056

Received: March 31, 2005; In Final Form: June 10, 2005

A method for calculating anharmonic vibrational energy levels in asymmetric top and linear systems that is based on second-order perturbation theory in curvilinear coordinates is extended to the bound generalized normal modes at nonstationary points along a reaction path. Explicit formulas for the anharmonicity coefficients, x_{ij}, and the constant term, E_0, are presented, and the necessary modifications for resonance cases are considered. The method is combined with variational transition state theory with semiclassical multidimensional tunneling approximations to calculate thermal rate constants for the HCN/HNC isomerization reaction. Although the results for this system are not very sensitive to the choice of coordinates, we find that the inclusion of anharmonicity leads to a substantial improvement in the vibrational energy levels. We also present detailed comparisons of rate constants computed with and without anharmonicity, with various approximations for incorporating tunneling along the reaction path, and with a more practical approach to calculating the vibrational partition functions needed for larger systems.

1. Introduction

For a given potential energy surface (PES), canonical variational transition state theory (CVT)[1−6] provides a practical method for calculating reliable thermal rate constants for a reacting system. Its application requires the evaluation of partition functions both for the reactant(s) and at a series of points along the reaction path, which we take here to be the minimum energy path (MEP), that is, the path of steepest descent in mass-scaled Cartesian coordinates starting from the saddle point.[3] The calculation of the partition functions is greatly simplified by assuming that the translational, rotational, vibrational, electronic, and reaction coordinate degrees of freedom are separable, and that the translational and rotational contributions can be treated using classical mechanics and the rigid rotor model.[7] The remaining degrees of freedom are treated quantum mechanically. In particular, the vibrational contribution to the rate constant at a point s along the MEP is given by the ratio of the vibrational partition function at s to that for the reactant(s), where the vibrational partition function, $Q_{vib}(T)$, at temperature T for a nonlinear species with N atoms is defined as

$$Q_{vib}(T) = \sum_{\mathbf{n}} \exp(-E_{\mathbf{n}}/kT) \qquad (1)$$

Here $E_{\mathbf{n}}$ is the energy of a vibrational level (relative to the bottom of the vibrational well) with a collection of quantum numbers indicated by $\mathbf{n}$, k is Boltzmann's constant, and the summation is carried out over the degrees of freedom corresponding to the "bound mode" vibrations. For a reactant, these $3N - 6$ degrees of freedom are the true bound vibrational modes of the species, whereas for a point along the MEP, these $3N - 7$ degrees of freedom are generalized normal modes representing the "bound" internal motions of the reacting complex that are locally orthogonal to the motion along the reaction path. (For a linear species, $3N - 6$ should be changed to $3N - 5$.) Thus, the energy levels of these modes directly affect the calculated reaction rate constant through the partition function in eq 1, whereas the zero point energy of these degrees of freedom determines the vibrationally adiabatic ground-state potential energy curve that is used to incorporate quantal effects (e.g., tunneling) into the description of the reaction coordinate degree of freedom.[3,8−11]

Because the calculation of the generalized normal modes requires that the reaction coordinate degree of freedom be projected out of the vibrational space at nonstationary points, the generalized normal-mode frequencies depend on the choice of coordinate system.[12−14] Rectilinear (e.g., Cartesian) coordinates, which have generally been the standard choice for the application of reaction-path methods to polyatomic systems,[3,15−21] can lead to imaginary harmonic frequencies.[12,13] However, physically reasonable results are obtained when the generalized normal modes are expressed in curvilinear coordinates,[12,13,22] (e.g., bond stretches and angle bends). In addition, the widely used harmonic approximation, which leads to very simple formulas for the vibrational energy levels and partition functions, can be innaccurate.[5−7,23−27] To include anharmonicity along the reaction path (as well as at stationary points) in a fashion that is consistent with curvilinear coordinate generalized normal modes, we herein make use of second-order perturbation theory in curvilinear coordinates.[28] This approach, which we denote as PT2C and which has been shown to provide fairly accurate vibrational energy levels in bound molecules,[29−32] takes into account both kinetic and potential anharmonic contributions.

Another consideration is that evaluating $Q_{vib}(T)$ by direct summation over anharmonic energy levels, as implied in eq 1, is not practical for systems containing more than a few atoms because the number of terms becomes prohibitive as N increases. In addition, the breakdown of perturbation theory for high-energy states may be severe.[5,24,26,33] To circumvent these problems, Truhlar and this author proposed a method, called

† Part of the special issue "Donald G. Truhlar Festschrift".

* Corresponding author. E-mail: isaacsad@muohio.edu.

10.1021/jp058113y CCC: $33.50
Published on Web 08/06/2005

simple perturbation theory (SPT),[34] in which $Q_{vib}(T)$ is approximated by

$$Q_{vib}(T) = \frac{e^{-\epsilon_0/kT}}{\prod_{i=1}^{3N-6}(1 - e^{-\Delta_i/kT})} \quad (2)$$

where the ground-state energy, ϵ_0, and the fundamental excitation energies, $\{\Delta_i, i = 1, ..., 3N - 6\}$, are evaluated by second-order perturbation theory in Cartesian coordinates (denoted simply as PT2). Those authors showed that this approach worked quite well in several cases of nonlinear systems containing from two to six modes.[5,34,35] In addition, this author showed that SPT is roughly as accurate as direct summation over PT2 energy levels for the HCN molecule and at the saddle point for the HCN/HNC isomerization reaction.[7]

In this paper, our preliminary investigation of the HCN/HNC isomerization reaction[7] is extended to the calculation of CVT rate constants, both with and without semiclassical transmission coefficients to account for reaction-coordinate tunneling. Below we first compare harmonic results obtained with rectilinear coordinates and with curvilinear coordinates. We then compare rate constants obtained from eq 1 with harmonic energy levels and with anharmonic levels. Finally, we compare rate constants obtained by direct summation over anharmonic energy levels and by SPT. All of the calculations reported herein were carried out with the widely used PES of Murrell, Carter, and Halonen (MCH).[36] Although this is not an accurate PES (e.g., the isomerization barrier of 12 168 cm^{-1} is too low, and there is an anomalous local maximum along the reaction path on the product side of the saddle point),[37,38] it is a global analytic PES that describes the entire HCN/HNC isomerization process. Thus, it should provide reasonable results for the rate constant comparisons outlined above. Section 2 describes the second-order perturbation theory calculation of the vibrational energy levels in curvilinear coordinates (PT2C) along a reaction path as well as for bound species, and the calculations for HCN and HNC as well as at the saddle point for the isomerization reaction are discussed in section 3. Selected details of the rate constant calculations are given in section 4, and the results are presented in section 5. Our conclusions are summarized in section 6.

2. Theory

Generalized Normal-Mode Analysis in Curvilinear Coordinates. Along a reaction path, the first derivatives of the potential energy are nonzero except at stationary points. Thus, to carry out a generalized normal-mode analysis at an arbitrary point along the reaction path, one must first project out from the second derivatives the first derivative contributions. This yields generalized vibrational frequencies (ω_i) as well as generalized normal modes (Q_i) that are linear combinations of the curvilinear coordinates (θ_t):

$$\theta_t = \sum_i L_{ti} Q_i \quad (3)$$

These generalized vibrational frequencies and normal modes are determined in the "spectroscopists units" used below (wherein both frequency and energy have units of cm^{-1}) as follows. Starting from the standard **G** and **F** matrices of Wilson, Decius, and Cross,[39] we define $\mathbf{G}' = h\mathbf{G}/4\pi^2 c$ and $\mathbf{F}' = \mathbf{F}/hc$. Then, following Jackels et al.,[13] at a point along the reaction path we define the projected force constant matrix

$$\mathbf{f}'^P = [1 - \mathbf{Gp}]^T \mathbf{F}'[1 - \mathbf{Gp}] \quad (4)$$

where, if **b** is the gradient in curvilinear coordinates, $\mathbf{p} = \mathbf{bb}^T/\mathbf{b}^T\mathbf{Gb}$. The nonzero eigenvalues and corresponding eigenvectors of the nonsymmetrical $\mathbf{G}'\mathbf{f}'^P$ matrix are then obtained as discussed in Jackels et al.:[13]

$$\mathbf{G}'\mathbf{f}'^P\Lambda = \Lambda\Omega \quad (5)$$

The square root of the positive eigenvalue Ω_{ii} is equal to the generalized normal-mode frequency ω_i in cm^{-1}, and the ith column of the Λ matrix is the corresponding unnormalized generalized normal mode. When normalized as outlined in Jackels et al.,[13] we obtain the normalized generalized normal mode coefficients L_{ti}, which have units of $cm^{1/2}$ if θ_t is a stretch and $cm^{-1/2}$ if θ_t is a bend.

Vibrational Energy Levels. Both potential and kinetic anharmonic contributions must be considered in order to calculate anharmonic vibrational levels of a *nonrotating* system within the space of the bound curvilinear generalized normal modes.[28,30] To see this, we express the pure vibrational Hamiltonian in terms of the generalized curvilinear normal coordinates, Q_i, and the conjugate momenta, P_i, as[30,40]

$$H = \frac{1}{2}\sum_{i,j} P_i \mu_{ij} P_j + V + V' \quad (6)$$

where, within the context of second-order perturbation theory discussed below, V' is a constant depending on the geometry and is discussed at the end of this section,

$$\mu_{ij} = \delta_{ij} + \sum_k \left(\frac{\partial g_{ij}}{\partial Q_k}\right) Q_k + \sum_{k,l} \left(\frac{\partial^2 g_{ij}}{\partial Q_k \partial Q_l}\right) Q_k Q_l \quad (7)$$

$$V = \frac{1}{2}\sum_k \omega_k^2 Q_k^2 + \sum_{i \le j \le k} f_{ijk} Q_i Q_j Q_k + \sum_{i \le j \le k \le l} f_{ijkl} Q_i Q_j Q_k Q_l \quad (8)$$

(All summations in this paper are unrestricted unless otherwise indicated.) Here g_{ij} is an element of the $\mathbf{G}'$ matrix transformed to

curvilinear normal coordinates so that

$$\left(\frac{\partial g_{ij}}{\partial Q_k}\right) = \sum_{r,s,t}\left(\frac{\partial \mathbf{G}'_{rs}}{\partial \theta_t}\right) L_{ir}^{-1} L_{js}^{-1} L_{tk} \tag{9}$$

$$\left(\frac{\partial^2 g_{ij}}{\partial Q_k \partial Q_l}\right) = \frac{1}{2}\sum_{r,s,t,u}\left(\frac{\partial^2 \mathbf{G}'_{rs}}{\partial \theta_t \partial \theta_u}\right) L_{ir}^{-1} L_{js}^{-1} L_{tk} L_{ul} \tag{10}$$

while f_{ijk} and f_{ijkl} are third- and fourth-order force constants along the normal modes, that is

$$f_{ijk} = (N_{\mathrm{ijk}})^{-1}\sum_{r,s,t}\left(\frac{\partial^3 V}{\partial \theta_r \partial \theta_s \partial \theta_t}\right) L_{ri} L_{sj} L_{tk} \tag{11}$$

$$f_{ijkl} = (N_{ijkl})^{-1}\sum_{r,s,t,u}\left(\frac{\partial^4 V}{\partial \theta_r \partial \theta_s \partial \theta_t \partial \theta_u}\right) L_{ri} L_{sj} L_{tk} L_{ul} \tag{12}$$

where N_{ijk} and N_{ijkl} are integers that depend on the number of identical subscripts.[28]

To use second-order perturbation theory to obtain anharmonic vibrational energy levels, we write

$$H = H^{(0)} + \lambda H^{(1)} + \lambda^2 H^{(2)} + V' \tag{13}$$

where, for the specific case of an *asymmetric top*[28]

$$H^{(0)} = \frac{1}{2}\sum_i P_i^2 + \frac{1}{2}\sum_i \omega_i^2 Q_i^2 \tag{14}$$

$$H^{(1)} = \frac{1}{2}\sum_{i,j,k}\left(\frac{\partial g_{ij}}{\partial Q_k}\right) Q_k P_i P_j + \sum_{i\le j\le k} f_{ijk} Q_i Q_j Q_k \tag{15}$$

$$H^{(2)} = \frac{1}{2}\sum_{i,j,k,l}\left(\frac{\partial^2 g_{ij}}{\partial Q_k \partial Q_l}\right) Q_k Q_l P_i P_j + \sum_{i\le j\le k\le l} f_{ijkl} Q_i Q_j Q_k Q_l \tag{16}$$

The operator $H^{(0)}$ is the standard Hamiltonian for uncoupled harmonic oscillators; its eigenvalues and eigenfunctions are

$$E_{\mathbf{n}}^{(0)} = \sum_i \omega_i\left(n_i + \frac{1}{2}\right) \text{ and } \Psi_{\mathbf{n}}^{(0)} = \prod_i \psi_{n_i}(Q_i) \tag{17}$$

where $\psi_{n_i}(Q_i)$ is the one-dimensional harmonic oscillator eigenfunction and $\mathbf{n}$ is the collection of n_i values.

From nondegenerate second-order perturbation theory, the vibrational energy of level $\mathbf{n}$ is given by

$$E_{\mathbf{n}} = E_{\mathbf{n}}^{(0)} + \langle \mathbf{n}|H^{(1)} + H^{(2)}|\mathbf{n}\rangle + \sum_{\mathbf{m}\neq\mathbf{n}} \frac{\langle \mathbf{n}|H^{(1)}|\mathbf{m}\rangle\langle \mathbf{m}|H^{(1)}|\mathbf{n}\rangle}{E_{\mathbf{n}}^{(0)} - E_{\mathbf{m}}^{(0)}} \tag{18}$$

where $|\mathbf{n}\rangle$ represents $|\Psi_{\mathbf{n}}^{(0)}\rangle$. Once the matrix elements have been evaluated,[41] $E_{\mathbf{n}}$ can be written as

$$E_{\mathbf{n}} = E_0 + \sum_i \omega_i\left(n_i + \frac{1}{2}\right) + \sum_{i,j} x_{ij}\left(n_i + \frac{1}{2}\right)\left(n_j + \frac{1}{2}\right) \tag{19}$$

where, using the notation

$$g_{ij,k} \equiv \left(\frac{\partial g_{ij}}{\partial Q_k}\right) \text{ and } g_{ij,kl} \equiv \left(\frac{\partial^2 g_{ij}}{\partial Q_k \partial Q_l}\right) \tag{20}$$

we find that[28]

$$x_{ii} = \frac{1}{4}g_{ii,ii} + \frac{3}{2}f_{iiii}\omega_i^{-2} - \frac{3}{16}g_{ii,i}^2 - \frac{15}{4}f_{iii}^2\omega_i^{-4} - \frac{3}{4}g_{ii,i}f_{iii}\omega_i^{-2} - \sum_{j\neq i}(4\omega_i^2 - \omega_j^2)^{-1}\left[\frac{1}{16}g_{ii,j}^2\omega_i^2\omega_j^{-2}(8\omega_i^2 - 3\omega_j^2) + \frac{1}{2}g_{ii,j}g_{ij,i}\omega_i^2 - \frac{1}{4}g_{ij,i}^2\omega_j^2 + \frac{1}{4}f_{iij}^2\omega_i^{-2}\omega_j^{-2}(8\omega_i^2 - 3\omega_j^2) + \frac{1}{4}g_{ii,j}f_{iij}\omega_j^{-2}(8\omega_i^2 - \omega_j^2) - g_{ij,i}f_{iij}\right] \quad (21)$$

$$x_{ij} = \frac{1}{2}g_{ii,jj}\omega_i\omega_j^{-1} + \frac{1}{2}f_{iijj}\omega_i^{-1}\omega_j^{-1} - \frac{1}{4}g_{ii,i}g_{jj,i}\omega_i^{-1}\omega_j - 3f_{iii}f_{ijj}\omega_i^{-3}\omega_j^{-1} - \frac{1}{2}g_{ii,i}f_{ijj}\omega_i^{-1}\omega_j^{-1} - \frac{3}{2}g_{jj,i}f_{iii}\omega_i^{-3}\omega_j - \frac{1}{8}\sum_{k\neq i,j}[g_{ii,k}g_{jj,k}\omega_i\omega_j\omega_k^{-2} + 4f_{iik}f_{jjk}(\omega_i\omega_j\omega_k^2)^{-1} + 4g_{ii,k}f_{jjk}\omega_i\omega_j^{-1}\omega_k^{-2}] - 2(4\omega_i^2 - \omega_j^2)^{-1}\left[\frac{1}{4}g_{ii,j}^2\omega_i^3\omega_j^{-1} + g_{ij,i}^2\omega_i\omega_j - \frac{1}{2}g_{ii,j}g_{ij,i}\omega_i\omega_j + f_{iij}^2\omega_i^{-1}\omega_j^{-1} - g_{ii,j}f_{iij}\omega_i\omega_j^{-1} + g_{ij,i}f_{iij}\omega_i^{-1}\omega_j\right] - \frac{1}{4}\sum_{k\neq i,j}D_{ijk}^{-1}\{[g_{ij,k}^2\omega_i\omega_j + g_{jk,i}^2\omega_i^{-1}\omega_j\omega_k^2 + g_{ik,j}^2\omega_i\omega_j^{-1}\omega_k^2](\omega_k^2 - \omega_i^2 - \omega_j^2) + 2g_{ij,k}g_{jk,i}\omega_i\omega_j(\omega_i^2 - \omega_j^2 - \omega_k^2) + 2g_{ij,k}g_{ik,j}\omega_i\omega_j(\omega_j^2 - \omega_i^2 - \omega_k^2) + 4g_{jk,i}g_{ik,j}\omega_i\omega_j\omega_k^2 + f_{ijk}^2\omega_i^{-1}\omega_j^{-1}(\omega_k^2 - \omega_i^2 - \omega_j^2) - 4g_{ij,k}f_{ijk}\omega_i\omega_j - 2g_{jk,i}f_{ijk}\omega_i^{-1}\omega_j(\omega_j^2 - \omega_i^2 - \omega_k^2) - 2g_{ik,j}f_{ijk}\omega_i\omega_j^{-1}(\omega_i^2 - \omega_j^2 - \omega_k^2)\} \quad (22)$$

with $D_{ijk} = (\omega_i + \omega_j + \omega_k)(\omega_i - \omega_j + \omega_k)(\omega_i + \omega_j - \omega_k)(\omega_i - \omega_j - \omega_k)$. The constant term, E_0, which is of no importance in spectroscopy and was not considered by Quade,[28] is necessary for the absolute values of the energy levels, and hence, for the partition functions. It is given by

$$E_0 = \sum_i\left[-\frac{3}{16}g_{ii,ii} + \frac{3}{8}f_{iiii}\omega_i^{-2} - \frac{3}{64}g_{ii,i}^2 - \frac{7}{16}f_{iii}^2\omega_i^{-4} + \frac{1}{16}g_{ii,i}f_{iii}\omega_i^{-2}\right] + \sum_{j\neq i}(4\omega_i^2 - \omega_j^2)^{-1}\left[\frac{3}{64}g_{ii,j}^2\omega_i^2 - \frac{3}{8}g_{ii,j}g_{ij,i}\omega_i^2 + \frac{3}{16}g_{ij,i}^2\omega_j^2 + \frac{3}{16}f_{iij}^2\omega_i^{-2} - \frac{3}{16}g_{ii,j}f_{iij} + \frac{3}{4}g_{ij,i}f_{iij}\right] - \frac{1}{16}\sum_{i\neq j\neq k}D_{ijk}^{-1}[2g_{ij,k}^2\omega_i^2\omega_j^2 + g_{ij,k}g_{jk,i}\omega_j^2(\omega_j^2 - \omega_i^2 - \omega_k^2) + g_{ij,k}g_{ik,j}\omega_i^2(\omega_i^2 - \omega_j^2 - \omega_k^2)] - \frac{1}{4}\sum_{i<j<k}D_{ijk}^{-1}[f_{ijk}^2 - g_{ij,k}f_{ijk}(\omega_k^2 - \omega_i^2 - \omega_j^2) - g_{ik,j}f_{ijk}(\omega_j^2 - \omega_i^2 - \omega_k^2) - g_{jk,i}f_{ijk}(\omega_i^2 - \omega_j^2 - \omega_k^2)] \quad (23)$$

To use second-order perturbation theory to obtain anharmonic vibrational energy levels for a *linear* species, we again write

$$H = H^{(0)} + \lambda H^{(1)} + \lambda^2 H^{(2)} + V' \quad (24)$$

where, with *i*, *j*, *k*, and *r* referring to nondegenerate modes and *s* and *t* each referring to a pair of doubly degenerate modes, the terms that contribute to the vibrational energy of a linear species are[28]

$$H^{(0)} = \frac{1}{2}\sum_r(P_r^2 + \omega_r^2Q_r^2) + \frac{1}{2}\sum_s(P_s^2 + Q_s^{-2}P_{\chi_s}^2 + \omega_s^2Q_s^2) \quad (25)$$

$$H^{(1)} = \frac{1}{2}\sum_{r,s,t}g_{st,r}Q_r(P_s^cP_t^c + P_s^sP_t^s) + \frac{1}{2}\sum_{r,s,t}g_{sr,t}P_r(Q_t^cP_s^c + Q_t^sP_s^s) + \sum_{i\leq j\leq k}f_{ijk}Q_iQ_jQ_k + \sum_{r,s\leq t}f_{rst}(Q_s^cQ_t^c + Q_s^sQ_t^s)Q_r \quad (26)$$

$$H^{(2)} = \frac{1}{2}\sum_s(g_{ss,ss}Q_s^2P_s^2 + A_{ss,ss}^{zz}P_{\chi_s}^2) + \frac{1}{2}\sum_{r,s}g_{rr,ss}Q_s^2P_r^2 + \frac{1}{2}\sum_{r,s}g_{ss,rr}Q_r^2(P_s^2 + Q_s^{-2}P_{\chi_s}^2) + \frac{1}{2}\sum_{s\neq t}g_{ss,tt}Q_t^2(P_s^2 + Q_s^{-2}P_{\chi_s}^2) + \sum_{a\leq b}f_{aabb}Q_a^2Q_b^2 \quad (27)$$

Here *a* and *b* can refer to either nondegenerate or degenerate modes; for a degenerate pair of modes, both polar, (Q_s, χ_s), and Cartesian, (Q_s^c, Q_s^s), representations have been used, where

$$Q_s^c = \cos\chi_s Q_s,\ Q_s^s = \sin\chi_s Q_s,\ P_s^c = \cos\chi_s P_s - \sin\chi_s Q_s^{-1}P_{\chi_s},\ \text{and } P_s^s = \sin\chi_s P_s + \cos\chi_s Q_s^{-1}P_{\chi_s} \quad (28)$$

The operator $H^{(0)}$ is again the standard Hamiltonian for uncoupled harmonic oscillators; its eigenvalues and eigenfunctions are

$$E_{\mathbf{n}}^{(0)} = \sum_a \omega_a\left(n_a + \frac{d_a}{2}\right) \text{ and } \Psi_{\mathbf{n}}^{(0)} = \prod_i \psi_{n_i}(Q_i)\prod_s \psi_{n_sl_s}(Q_s, \chi_s) \quad (29)$$

where $d_a = 1$ for a nondegenerate mode and $d_a = 2$ for a doubly degenerate mode, $\psi_{n_i}(Q_i)$ is a one-dimensional harmonic oscillator eigenfunction, and $\psi_{n_sl_s}(Q_s, \chi_s)$ is the polar representation of a two-dimensional isotropic oscillator; **n** is then the collection of n_i, n_s, and l_s values.

From degenerate second-order perturbation theory, the vibrational energy of level **n** is again given by[42]

$$E_{\mathbf{n}} = E_{\mathbf{n}}^{(0)} + \langle \mathbf{n}|H^{(1)} + H^{(2)}|\mathbf{n}\rangle + \sum_{\mathbf{m}\neq\mathbf{n}} \frac{\langle \mathbf{n}|H^{(1)}|\mathbf{m}\rangle\langle \mathbf{m}|H^{(1)}|\mathbf{n}\rangle}{E_{\mathbf{n}}^{(0)} - E_{\mathbf{m}}^{(0)}} \tag{30}$$

where $|\mathbf{n}\rangle$ represents $|\Psi_{\mathbf{n}}^{(0)}\rangle$ and where at least one of the n_i or n_s values differ in $|\mathbf{n}\rangle$ and $|\mathbf{m}\rangle$. (In principle, $E_{\mathbf{n}}$ should be determined by diagonalizing an energy matrix whose elements are given by the formula above, but with $|\mathbf{n}\rangle$ replaced by $|\mathbf{n}'\rangle$, where l_s', $l_t' = l_s$, l_t or l_s', $l_t' = l_s \pm 2$, $l_t \mp 2$. However, the latter case is only important for the *l*-doubling energy,[43] which has been omitted here and is unimportant for the zero point energy and the fundamentals. Thus, the equation above is written for the diagonal case only.) Matrix elements of the operators appearing in the above equation have been obtained in Hermitian form by multiplying the matrix representations of the basic operators given in the literature.[44−46] From these, $E_{\mathbf{n}}$ can be written as

$$E_{\mathbf{n}} = E_0 + \sum_a \omega_a\left(n_a + \frac{d_a}{2}\right) + \sum_{a,b} x_{ab}\left(n_a + \frac{d_a}{2}\right)\left(n_b + \frac{d_b}{2}\right) + \sum_{s,t} x_{l_s l_t} l_s l_t \tag{31}$$

where[28]

$$x_{ii} = \frac{3}{2} f_{iiii}\omega_i^{-2} - \frac{15}{4} f_{iii}^2\omega_i^{-4} - \sum_{j\neq i}(4\omega_i^2 - \omega_j^2)^{-1}\left[\frac{1}{4} f_{iij}^2\omega_i^{-2}\omega_j^{-2}(8\omega_i^2 - 3\omega_j^2)\right] \tag{32}$$

$$x_{ij} = \frac{1}{2} f_{iijj}\omega_i^{-1}\omega_j^{-1} - 3f_{iii}\, f_{ijj}\omega_i^{-3}\omega_j^{-1} - (4\omega_i^2 - \omega_j^2)^{-1}[2f_{iij}^2\omega_i^{-1}\omega_j^{-1}] - \sum_{k\neq i,j}\left\{\frac{1}{2} f_{iik}\, f_{jjk}(\omega_i\omega_j\omega_k^2)^{-1} + D_{ijk}^{-1}\left[\frac{1}{4} f_{ijk}^2\omega_i^{-1}\omega_j^{-1}(\omega_k^2 - \omega_i^2 - \omega_j^2)\right]\right\} \tag{33}$$

$$x_{ss} = \frac{1}{4} g_{ss,ss} + \frac{3}{2} f_{ssss}\omega_s^{-2} - \sum_r (4\omega_s^2 - \omega_r^2)^{-1}\left[\frac{1}{16} g_{ss,r}^2\omega_r^{-2}\omega_s^2(8\omega_s^2 - 3\omega_r^2) - \frac{1}{4} g_{sr,s}^2\omega_r^2 + \frac{1}{2} g_{ss,r}\, g_{sr,s}\omega_s^2 + \frac{1}{4} f_{rss}^2\omega_r^{-2}\omega_s^{-2}(8\omega_s^2 - 3\omega_r^2) + \frac{1}{4} g_{ss,r}\, f_{rss}\omega_r^{-2}(8\omega_s^2 - \omega_r^2) - g_{sr,s}\, f_{rss}\right] \tag{34}$$

$$x_{rs} = \frac{1}{4} g_{rr,ss}\omega_r\omega_s^{-1} + \frac{1}{4} g_{ss,rr}\omega_r^{-1}\omega_s + \frac{1}{2} f_{rrss}\omega_r^{-1}\omega_s^{-1} - \frac{3}{2} f_{rrr}\, f_{rss}\omega_r^{-3}\omega_s^{-1} - \frac{3}{4} g_{ss,r}\, f_{rrr}\omega_r^{-3}\omega_s - \frac{1}{4}\sum_{k\neq r}[2f_{rrk}\, f_{kss}(\omega_r\omega_k^2\omega_s)^{-1} + g_{ss,k}\, f_{rrk}\omega_r^{-1}\omega_k^{-2}\omega_s] - (4\omega_s^2 - \omega_r^2)^{-1}\left[\frac{1}{4} g_{ss,r}^2\omega_r^{-1}\omega_s^3 + g_{sr,s}^2\omega_r\omega_s - \frac{1}{2} g_{ss,r}\, g_{sr,s}\omega_r\omega_s + f_{rss}^2\omega_r^{-1}\omega_s^{-1} - g_{ss,r}\, f_{rss}\omega_r^{-1}\omega_s + g_{sr,s}\, f_{rss}\omega_r\omega_s^{-1}\right] - \sum_{t\neq s} D_{rst}^{-1}\left\{\frac{1}{4}[g_{sr,t}^2\omega_r\omega_s + g_{st,r}^2\omega_r^{-1}\omega_s\omega_t^2 + g_{tr,s}^2\omega_r\omega_s^{-1}\omega_t^2](\omega_t^2 - \omega_r^2 - \omega_s^2) + \frac{1}{2} g_{sr,t}\, g_{tr,s}\omega_r\omega_s(\omega_s^2 - \omega_r^2 - \omega_t^2) + \frac{1}{2} g_{st,r}\, g_{sr,t}\omega_r\omega_s(\omega_r^2 - \omega_s^2 - \omega_t^2) + g_{st,r}\, g_{tr,s}\omega_r\omega_s\omega_t^2 + \frac{1}{4} f_{rst}^2\omega_r^{-1}\omega_s^{-1}(\omega_t^2 - \omega_r^2 - \omega_s^2) - g_{sr,t}\, f_{rst}\omega_r\omega_s - \frac{1}{2} g_{st,r}\, f_{rst}\omega_r^{-1}\omega_s(\omega_s^2 - \omega_r^2 - \omega_t^2) - \frac{1}{2} g_{tr,s}\, f_{rst}\omega_r\omega_s^{-1}(\omega_r^2 - \omega_s^2 - \omega_t^2)\right\} \tag{35}$$

$$x_{st} = \frac{1}{2} g_{ss,tt}\omega_s\omega_t^{-1} + \frac{1}{2} f_{sstt}\omega_s^{-1}\omega_t^{-1} - \frac{1}{2}\sum_r\left[\frac{1}{4} g_{ss,r}\, g_{tt,r}\omega_r^{-2}\omega_s\omega_t + f_{rss}\, f_{rtt}(\omega_r^2\omega_s\omega_t)^{-1} + g_{tt,r}\, f_{rss}\omega_r^{-2}\omega_s^{-1}\omega_t)\right] - \sum_r D_{rst}^{-1}\left\{\left[\frac{1}{4} g_{sr,t}^2\omega_r^2\omega_s\omega_t^{-1} + \frac{1}{8} g_{st,r}^2\omega_s\omega_t\right](\omega_r^2 - \omega_s^2 - \omega_t^2) + \frac{1}{2} g_{sr,t}\, g_{tr,s}\omega_r^2\omega_s\omega_t + \frac{1}{4} g_{st,r}\, g_{sr,t}\omega_s\omega_t(\omega_t^2 - \omega_r^2 - \omega_s^2) + \frac{1}{4} g_{st,r}\, g_{tr,s}\omega_s\omega_t(\omega_s^2 - \omega_r^2 - \omega_t^2) + \frac{1}{8} f_{rst}^2\omega_s^{-1}\omega_t^{-1}(\omega_r^2 - \omega_s^2 - \omega_t^2) - \frac{1}{4} g_{sr,t}\, f_{rst}\omega_s\omega_t^{-1}(\omega_s^2 - \omega_r^2 - \omega_t^2) - \frac{1}{2} g_{st,r}\, f_{rst}\omega_s\omega_t - \frac{1}{4} g_{tr,s}\, f_{rst}\omega_s^{-1}\omega_t(\omega_t^2 - \omega_r^2 - \omega_s^2)\right\} \tag{36}$$

$$x_{l_s l_s} = -\frac{1}{4} g_{ss,ss} - \frac{1}{2} f_{ssss}\omega_s^{-2} - \sum_r (4\omega_s^2 - \omega_r^2)^{-1}\left[\frac{1}{16} g_{ss,r}^2\omega_s^2 + \frac{1}{4} g_{sr,s}^2\omega_r^2 - \frac{1}{2} g_{ss,r}\, g_{sr,s}\omega_s^2 + \frac{1}{4} f_{rss}^2\omega_s^{-2} - \frac{1}{4} g_{ss,r}\, f_{rss} + g_{sr,s}\, f_{rss}\right] \tag{37}$$

$$x_{l_s l_t} = \sum_r D_{rst}^{-1}\left[\frac{1}{2} g_{sr,t}^2\omega_r^2\omega_s^2 + \frac{1}{4} g_{st,r}^2\omega_s^2\omega_t^2 + \frac{1}{4} g_{sr,t}\, g_{tr,s}\omega_r^2(\omega_r^2 - \omega_s^2 - \omega_t^2) + \frac{1}{4} g_{st,r}\, g_{sr,t}\omega_s^2(\omega_s^2 - \omega_r^2 - \omega_t^2) + \frac{1}{4} g_{st,r}\, g_{tr,s}\omega_t^2(\omega_t^2 - \omega_r^2 - \omega_s^2) + \frac{1}{4} f_{rst}^2 - \frac{1}{4} g_{sr,t}\, f_{rst}(\omega_t^2 - \omega_r^2 - \omega_s^2) - \frac{1}{4} g_{st,r}\, f_{rst}(\omega_r^2 - \omega_s^2 - \omega_t^2) - \frac{1}{4} g_{tr,s}\, f_{rst}(\omega_s^2 - \omega_r^2 - \omega_t^2)\right] \tag{38}$$

$$E_0 = -\sum_s \left[\frac{1}{4} g_{ss,ss} - \frac{1}{2} f_{ssss}\omega_s^{-2}\right] + \sum_r \left[\frac{3}{8} f_{rrrr}\omega_r^{-2} - \frac{7}{16} f_{rrr}^2 \omega_r^{-4}\right] + \sum_{j\neq i} (4\omega_i^2 - \omega_j^2)^{-1}\left[\frac{3}{16} f_{iij}^2 \omega_i^{-2}\right] - \sum_{i<j<k} D_{ijk}^{-1}\left[\frac{1}{4} f_{ijk}^2\right] +$$
$$\sum_{r,s} (4\omega_s^2 - \omega_r^2)^{-1}\left[\frac{1}{16} g_{ss,r}^2 \omega_s^2 + \frac{1}{4} g_{sr,s}^2 \omega_r^2 - \frac{1}{2} g_{ss,r} g_{sr,s} \omega_s^2 + \frac{1}{4} f_{rss}^2 \omega_s^{-2} - \frac{1}{4} g_{ss,r} f_{rss} + g_{sr,s} f_{rss}\right] - \sum_{r,s\neq t} D_{rst}^{-1}\left[\frac{1}{2} g_{sr,t}^2 \omega_r^2 \omega_s^2 +\right.$$
$$\left. \frac{1}{4} g_{st,r}^2 \omega_s^2 \omega_t^2 + \frac{1}{4} g_{sr,t} g_{tr,s} \omega_r^2 (\omega_r^2 - \omega_s^2 - \omega_t^2) + \frac{1}{4} g_{st,r} g_{sr,t} \omega_s^2 (\omega_s^2 - \omega_r^2 - \omega_t^2) + \frac{1}{4} g_{st,r} g_{tr,s} \omega_t^2 (\omega_t^2 - \omega_r^2 - \omega_s^2)\right] -$$
$$\sum_{r<s<t} D_{rst}^{-1}\left[\frac{1}{2} f_{rst}^2 - \frac{1}{2} g_{st,r} f_{rst} (\omega_r^2 - \omega_s^2 - \omega_t^2) - \frac{1}{2} g_{sr,t} f_{rst} (\omega_t^2 - \omega_r^2 - \omega_s^2) - \frac{1}{2} g_{tr,s} f_{rst} (\omega_s^2 - \omega_r^2 - \omega_t^2)\right] \quad (39)$$

Note that in applying these equations, $(x_{rs} + x_{sr})$ should be replaced by $2x_{rs}$.[47]

The V' term in the Hamiltonian (cf. eqs 13 and 24) arises from the noncommutativity of the position and momentum operators; it is evaluated as follows. For a nonlinear molecule, it is given (in cm^{-1}) by[30,48]

$$V' = \frac{\hbar}{16\pi c} \sum_{i,j} \left\{ \left(\frac{\partial G_{ij}}{\partial \theta_i}\right)\left(\frac{\partial \ln \Gamma}{\partial \theta_j}\right) + G_{ij}\left[\left(\frac{\partial^2 \ln \Gamma}{\partial \theta_i \partial \theta_j}\right) + \frac{1}{4}\left(\frac{\partial \ln \Gamma}{\partial \theta_i}\right)\left(\frac{\partial \ln \Gamma}{\partial \theta_j}\right)\right]\right\} \quad (40)$$

where Γ is the ratio of the determinants of the moment of inertia tensor and **G**, $\Gamma = |\mathbf{I}|/|\mathbf{G}|$. For a linear bound ABC system, the singularities in V' can be removed by a change of variables;[30] the result is

$$V' = \frac{\hbar}{2\pi c}\left(\frac{1}{m_B r_1 r_2} - \frac{G_{bb}}{6}\right) \quad (41)$$

where r_1, r_2 are the AB and BC distances, respectively, and G_{bb} is the bend−bend element of the **G** matrix. Along the reaction path, the expression for V' must be restricted to the *bound* curvilinear normal coordinates Q_i

$$V' = \frac{1}{8} \sum_{\substack{i,j \\ \text{bound}}} \left\{ \left(\frac{\partial g_{ij}}{\partial Q_i}\right)\left(\frac{\partial \ln \gamma}{\partial Q_j}\right) + g_{ij}\left[\left(\frac{\partial^2 \ln \gamma}{\partial Q_i \partial Q_j}\right) + \frac{1}{4}\left(\frac{\partial \ln \gamma}{\partial Q_i}\right)\left(\frac{\partial \ln \gamma}{\partial Q_j}\right)\right]\right\} \quad (42)$$

where the **g** matrix is obtained by transforming the $\mathbf{G}'$ matrix to normal coordinates

$$g_{ij} = \sum_{m,n} \boldsymbol{G}'_{mn} L_{im}^{-1} L_{jn}^{-1} \quad (43)$$

and where $\gamma = |\mathbf{I}|/|\mathbf{g}|$. This expression for V' is efficiently evaluated numerically using finite-difference methods for the derivatives.

Anharmonic Resonance. Along a reaction path, the generalized frequencies change continuously. Thus, at some point on the path, it is possible that $2\omega_i \approx \omega_j$ for a pair of frequencies, or that $\omega_i + \omega_j \approx \omega_k$ for a triplet of frequencies. (Of course, the same situation arises in certain bound molecules.[49−51]) In such resonance situations, the accidental near degeneracy of two or more unperturbed (harmonic) vibrational energy levels relative to the interaction force constant that couples them can cause a breakdown of perturbation theory, as some terms in eqs 21−23 and eqs 32−39 may blow up. (We define *iij*- or *ijk*-type interactions to be resonant if the $|f_{iij}/[\omega_i \omega_j^{1/2}(2\omega_i - \omega_j)]|$ ratio or the $|f_{ijk}/[(\omega_i\omega_j\omega_k)^{1/2}(\omega_i + \omega_j - \omega_k)]|$ ratio, respectively, exceeds a minimum value, *p*. A value for *p* of 0.20 has been found to distinguish between resonant and nonresonant interactions.[5,6,26]) In these cases, one first removes the resonant contributions[49,50] from the energy levels of asymmetric top or linear systems by making the replacements in the anharmonicity coefficients and in E_0 that are given by eqs S44 to S74 in the Supporting Information. These substitutions yield "deperturbed" vibrational energy levels.[52] If desired, the resonant levels can be improved by including the coupling between the degenerate levels directly. However, this has been shown to have little effect on the resulting vibrational partition function[26] and was not done here.

3. Vibrational Energy Levels

Along the reaction path for the HCN/HNC isomerization, the system is described by three internal coordinates, two bond stretches and a nonlinear bend, whereas for HCN and HNC, the system is described by four internal coordinates, two bond stretches and two linear bends. All of the internal coordinates were expressed in difference Cartesians as discussed in Jackels et al.,[13] except the linear bending coordinates were defined as the arcsine of the expressions given in eqs 34a and b of that work so that these coordinates would be true angles measured in radians. The **G** matrix was then constructed as in Jackels et al.,[13] but the **F** matrix was evaluated by direct numerical differentiation in internal coordinates of the analytic gradient in internals, as were the higher-order derivatives of the potential energy. Direct numerical differentiation in internals was also used for the derivatives of the **G** matrix.

For HCN and HNC, the normal-mode analysis yields four bound modes, two stretches and a doubly degenerate bend. Each vibrational state of these linear species can thus be labeled by four approximate quantum numbers and denoted as $v_1 v_2^l v_3$, where v_1, v_2, and v_3 are associated with the CN stretch, the degenerate bend, and the CH or NH stretch, respectively, and where, for given v_2, the vibrational angular momentum quantum number l can take on the values v_2, $v_2 - 2$, ..., $-v_2 + 2$, $-v_2$.[7] For a point on the MEP, however, the generalized normal-mode analysis discussed above yields two bound modes that mainly involve the two stretching motions; the bending motion roughly corresponds to motion along the reaction path. Each generalized

TABLE 1: Zero Point Energy[a] and Fundamentals[b] (in cm^{-1}) for HCN, HNC, and at the Saddle Point

level	harmonic	PT2	PT2C	accurate
		HCN		
00^00	3520.88	3480.83	3485.26	3483.24
10^00	2127.46	2097.26	2097.38	2096.89
01^10	731.71	715.41	714.93	719.95
00^01	3450.89	3308.67	3315.81	3318.56
		HNC		
00^00	3422.33	3377.34	3383.75	3380.21
10^00	2060.88	2029.25	2029.52	2029.88
01^10	494.05	481.56	482.59	483.67
00^01	3795.68	3620.09	3631.54	3632.45
		saddle point		
00	2676.32	2647.60	2647.40	2647.25
10	2223.53	2157.66	2157.50	2149.70
01	3129.11	3002.08	3001.76	3001.29

[a] Measured from the bottom of the corresponding vibrational well. [b] Measured relative to the zero point energy.

bound vibrational state is then labeled by just two quantum numbers and denoted as v_1v_2, where v_1 and v_2 are associated with the CN stretch and the stretch of the hydrogen relative to the CN bond, respectively.

Considering the potential effects of resonance for this system, we found that for all cubic interactions, the $|f_{iij}/[\omega_i\omega_j^{1/2}(2\omega_i - \omega_j)]|$ ratio is no larger than 0.08, except for the f_{113} interaction in HNC, for which it is 0.22. Because removing the f_{113} contribution from the vibrational energy affects only the excited states,[35] treating this interaction as resonant affects only the rate constant for the reverse reaction. In fact, numerical tests demonstrate that removing this interaction raises the 00^01 HNC fundamental by 4.0 cm^{-1} and changes the reverse rate constants in at most the fourth significant figure for the temperatures considered here (200−4000 K). Choosing the value of p to be 0.07 also treats the f_{122} interaction along the MEP as resonant, which affects the generalized excited states and vibrational partition function for the generalized transition state. However, removing this interaction does not change the rate constants to three significant figures. Thus, all of the results quoted in this paper include all cubic interactions, that is, no interactions have been removed.

Table 1 lists the accurate zero point energy and fundamentals for HCN, HNC, and at the saddle point for the HCN/HNC isomerization on the MCH surface.[36] As discussed previously,[7] these were obtained for HCN and HNC from discrete variable calculations with the DVR3D suite of programs,[53] whereas those for the saddle point were obtained from the vibrational SCF-CI method with the POLYMODE program.[54] These values agree quite well with those computed by perturbation theory in rectilinear coordinates (PT2)[7] and in curvilinear coordinates (PT2C, present work). In fact, the average absolute error in the zero point energies is only 1.9 cm^{-1} for both approximate approaches, whereas the average absolute errors in the fundamentals is 4.8 cm^{-1} for PT2 and 2.4 cm^{-1} for PT2C. (It should be noted that the present PT2C results for HCN are in almost exact agreement with those reported in ref 30. In addition, as noted in that work, if the same Hamiltonian is used in both cases, rectilinear and curvilinear coordinates lead to identical perturbation theory energy levels when no resonances are removed,[30] as is the case here. The differences between the present PT2 and PT2C results are likely due to the neglect of small vibrational angular momentum terms in the usual application of perturbation theory to the Hamiltonian in rectilinear coordinates.[49,50]) In contrast, the harmonic approximation leads to fairly large errors: on average, the zero point energies are too high by 36 cm^{-1} and the fundamentals are too high by 73 cm^{-1}, with the errors in the fundamentals involving the hydrogen stretch being particularly large. Thus, we would expect the vibrational partition functions (and, hence, the rate constants) derived from the perturbation theory levels to be fairly accurate, whereas we expect the error in the vibrational partition functions obtained from the harmonic levels to be significant, as discussed before.[7]

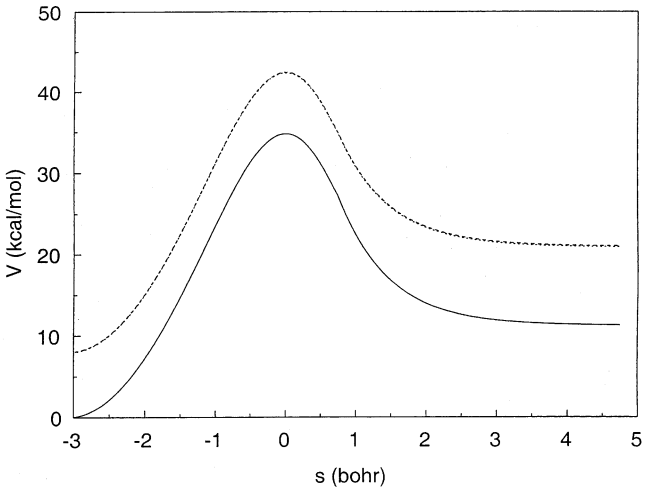

Figure 1. Calculated classical potential energy, V_{MEP} (solid curve), and ground-state vibrationally adiabatic potential energy, V_a^G (dashed curve, harmonic; dotted curve, anharmonic), as functions of the reaction coordinate, s.

4. Rate Constant Calculations

Figure 1 shows the classical potential energy curve (V_{MEP}) and two ground-state vibrationally adiabatic potential energy curves (V_a^G) along the reaction path. The reaction coordinate, s, is defined as the signed distance along the MEP from the saddle point ($s = 0$) to HCN ($s < 0$) and HNC ($s > 0$) through mass-scaled Cartesian coordinates, where the coordinates are scaled to a reduced mass of 1 amu.[2] The solid curve, $V_{MEP}(s)$, is the Born−Oppenheimer potential energy along the reaction path, whereas the two upper curves, $V_a^G(s)$, are sums of $V_{MEP}(s)$ and the total zero point energy for the bound vibrational degrees of freedom orthogonal to the MEP at s. For the dashed (upper) curve, the zero point energy was computed harmonically, whereas for the dotted (lower) curve it was calculated by the PT2C approach discussed above. We note in passing that projecting out the reaction coordinate direction in rectilinear coordinates and using the PT2 approach in place of PT2C would not change the energies of these curves by more than 0.02 kcal/mol. We also note that the curves in Figure 1 have been obtained from the actual MCH potential energy function only up to $s = 0.75$ bohr. For $s > 0.75$ bohr, the actual MCH potential energy function exhibits a local minimum along the reaction path. Thus, we extrapolated the energy curves for $s > 0.75$ bohr to their HNC limits by simple exponential functions, as discussed elsewhere.[2] Fitting the exponentials to the actual energy curves at $s = 0.75$ bohr yields an exponential range parameter of $\alpha = 1.1$ bohr^{-1}. Because this value of α produced energy curves that appeared to decay too slowly, the value of α was arbitrarily changed to 1.4 bohr^{-1} to better represent the true situation in this system. To examine the sensitivity of the results on the choice of α, below we compare rate constants obtained with $\alpha = 1.4$ bohr^{-1} and with $\alpha = 1.1$ bohr^{-1}. When the curvature of the MEP is neglected, the $V_a^G(s)$ curve provides an effective barrier for reaction path tunneling.[3,8,9] Thus, we find below that,

at low temperature, the choice of α has a large effect on rate constants that include tunneling. However, given the closeness of the $V_a^G(s)$ curves for which the zero point energy is computed harmonically or by the PT2C approach, we expect that the inclusion of anharmonicity will only have a mild effect on the rate constant, as shown below.

CVT rate constants for the HCN/HNC isomerization reaction were obtained exactly as described previously.[2] For results that are converged to at least three significant figures, the MEP was computed by the Euler single-step method[3,55] with a step size between gradient calculations of 0.0001 bohr and a distance between generalized normal mode calculations of 0.005 bohr. The generalized transition state was optimized for each temperature by finding the maximum of the generalized free energy of activation with respect to the reaction coordinate. For comparison, we also calculated conventional transition state theory (TST) rate constants, which result from locating the transition state at the saddle point ($s = 0.0$). The vibrational partition function at temperature T was computed either by direct summation over the vibrational levels (eq 1) up to the lowest dissociation energy of the system (45 676 cm^{-1}) or by the SPT approach (eq 2). Quantum effects along the reaction coordinate degree of freedom, which account for hydrogen tunneling, were included by multiplying the CVT rate constant by one of two semiclassical adiabatic ground-state (SAG) transmission coefficients.[1,3,9] The MEPSAG transmission coefficient[3,8−10] is based on tunneling along the MEP, whereas the centrifugal-dominant small-curvature (CD-SCSAG) transmission coefficient[11,56] includes the curvature-coupling of the reaction path to the generalized normal modes of the transition state. The CD-SCSAG transmission coefficient thus allows for corner-cutting during tunneling and is more accurate.[57,58]

5. Rate Constant Results

For this PES, the variational effect is very small. In fact, although the location of the "dynamic bottleneck", that is, the value of s at which the generalized free energy of activation is a maximum, increases toward the product with increasing temperature, it remains less than 0.025 bohr up to the highest temperature considered in this study (4000 K). Because of this, the conventional (TST) and canonical variational transition state theory (CVT) rate constants are the same to three significant figures at all temperatures, so below we quote only the CVT results. Table 2 presents the rate constants for the HCN/HNC isomerization reaction calculated with various levels of approximation. The tabulated values are those computed using curvilinear internal coordinates, whereas the k_{curv}/k_{Cart} ratio of the rate constant computed using curvilinear coordinates to that computed using Cartesian coordinates is given in parentheses. For each temperature, the first line contains the harmonic results, whereas the values on the second line include the effects of anharmonicity through the PT2C approach discussed above. From the CVT values, we find that neglecting anharmonicity yields uniformly higher rate constants. Furthermore, at a given temperature the ratio of the harmonic to the anharmonic result is roughly the same whether reaction-path tunneling is included or excluded showing that the effect of neglecting anharmonicity on the ground-state adiabatic potential, $V_a^G(s)$, is much less important than the effect on the vibrational levels that lead to the vibrational partition functions. Because the CVT rate constant depends on the *ratio* of the vibrational partition function for the generalized transition state at the dynamic bottleneck to that for HCN, some of the error introduced by neglecting anharmonicity cancels out for this system.[7] Thus, the differences

TABLE 2: Calculated Rate Constants for the HCN/HNC Isomerization Reaction[a]

T (K)	CVT	CVT/MEPSAG	CVT/CD-SCSAG
200	7.69×10^{-23} (1.00)	1.01×10^{-19} (0.98)	4.06×10^{-19} (0.98)
	7.32×10^{-23} (1.03)	9.55×10^{-20} (1.01)	3.85×10^{-19} (1.01)
250	1.25×10^{-15} (1.00)	2.32×10^{-14} (0.99)	4.37×10^{-14} (0.99)
	1.20×10^{-15} (1.03)	2.21×10^{-14} (1.02)	4.18×10^{-14} (1.01)
298	5.74×10^{-11} (1.00)	2.98×10^{-10} (1.00)	4.02×10^{-10} (0.99)
	5.53×10^{-11} (1.02)	2.86×10^{-10} (1.02)	3.86×10^{-10} (1.02)
400	9.25×10^{-5} (1.00)	2.00×10^{-4} (1.00)	2.25×10^{-4} (1.00)
	8.94×10^{-5} (1.02)	1.93×10^{-4} (1.01)	2.17×10^{-4} (1.01)
600	1.06×10^{2} (1.00)	1.45×10^{2} (1.00)	1.52×10^{2} (1.00)
	1.03×10^{2} (1.01)	1.40×10^{2} (1.01)	1.47×10^{2} (1.01)
1000	7.37×10^{6} (1.00)	8.22×10^{6} (1.00)	8.34×10^{6} (1.00)
	7.08×10^{6} (1.00)	7.89×10^{6} (1.00)	8.00×10^{6} (1.00)
1500	1.86×10^{9} (1.00)	1.95×10^{9} (1.00)	1.96×10^{9} (1.00)
	1.77×10^{9} (1.00)	1.86×10^{9} (1.00)	1.87×10^{9} (1.00)
2400	1.11×10^{11} (1.00)	1.13×10^{11} (1.00)	1.13×10^{11} (1.00)
	1.03×10^{11} (0.99)	1.05×10^{11} (0.99)	1.05×10^{11} (0.99)
4000	1.55×10^{12} (1.00)	1.55×10^{12} (1.00)	1.56×10^{12} (1.00)
	1.37×10^{12} (0.97)	1.38×10^{12} (0.97)	1.38×10^{12} (0.97)

[a] Units are s^{-1}. For each temperature, upper entry is harmonic, whereas lower entry is anharmonic result. The k_{curv}/k_{Cart} or k_{PT2C}/k_{PT2} ratio is given in parentheses.

TABLE 3: CVT Rate Constants (in s^{-1}) for the HCN/HNC Isomerization Reaction

T (K)	PT2C	SPT
200	7.32×10^{-23}	7.32×10^{-23}
250	1.20×10^{-15}	1.20×10^{-15}
298	5.53×10^{-11}	5.53×10^{-11}
400	8.94×10^{-5}	8.94×10^{-5}
600	1.03×10^{2}	1.03×10^{2}
1000	7.08×10^{6}	7.13×10^{6}
1500	1.77×10^{9}	1.80×10^{9}
2400	1.03×10^{11}	1.07×10^{11}
4000	1.37×10^{12}	1.50×10^{12}

in the vibrational zero point energies lead to a harmonic rate constant that is about 5% higher than the corresponding anharmonic value at 200 K. This effect decreases to around 4% at 298 K, but differences in the excited vibrational levels cause a further increase in the difference between the harmonic and anharmonic results that becomes more pronounced with increasing temperature, reaching 13% at 4000 K. The parenthetical values in Table 2 also show that the rate constants obtained from this PES are not very sensitive to the choice of coordinates. As discussed above, the $V_a^G(s)$ curves obtained with either Cartesian or curvilinear coordinates are very close, and the corresponding calculated rate constants differ by no more than 3%. Finally, Table 2 shows that reaction-path tunneling is very important below 1000 K for this PES. For example, at 298 K the inclusion of tunneling along the MEP (CVT/MEPSAG vs CVT) raises the PT2C rate constant by a factor of 5.2, whereas additionally incorporating the curvature of the reaction path (CVT/CD-SCSAG vs CVT) raises the PT2C rate constant by a factor of 7.0, thereby yielding a more reliable estimate of the effects of tunneling on the rate constant.

Table 3 compares CVT rate constants computed from vibrational partition functions obtained by direct summation over the anharmonic vibrational levels (eq 1, PT2C) or by the SPT approach (eq 2). (Because the transmission coefficients are unaffected by the manner in which the vibrational partition function is calculated, a comparison of CVT/MEPSAG or CVT/CD-SCSAG rate constants would exhibit identical behavior.) These results show that there are negligible differences between the results of these methods for temperatures below 1000 K. Because both methods employ the same zero point energy, this result is not surprising. Above 1000 K, the difference in the

TABLE 4: HCN/HNC Isomerization Rate Constants for Different Exponential Range Parameters[a]

	CVT/MEPSAG		CVT/CD-SCSAG	
T (K)	$\alpha = 1.4$	$\alpha = 1.1$	$\alpha = 1.4$	$\alpha = 1.1$
200	1.01×10^{-19}	6.73×10^{-20}	4.06×10^{-19}	2.33×10^{-19}
	9.55×10^{-20}	6.38×10^{-20}	3.85×10^{-19}	2.21×10^{-19}
250	2.32×10^{-14}	2.24×10^{-14}	4.37×10^{-14}	4.06×10^{-14}
	2.21×10^{-14}	2.14×10^{-14}	4.18×10^{-14}	3.88×10^{-14}
298	2.98×10^{-10}	2.97×10^{-10}	4.02×10^{-10}	3.99×10^{-10}
	2.86×10^{-10}	2.86×10^{-10}	3.86×10^{-10}	3.84×10^{-10}
400	2.00×10^{-4}	2.00×10^{-4}	2.25×10^{-4}	2.25×10^{-4}
	1.93×10^{-4}	1.93×10^{-4}	2.17×10^{-4}	2.17×10^{-4}

[a] Units of rate constants are s^{-1}. For each temperature, upper entry is harmonic, whereas lower entry is anharmonic (PT2C) result.

treatment of the excited levels by the two approaches yield SPT rate constants that are higher than the PT2C ones by 2% at 1500 K, 4% at 2400 K, and 9% at 4000 K. As discussed previously,[7] the SPT results are more accurate for this system at high temperature because of errors in the perturbation theory estimates for the energies of the highly excited vibrational states. In addition, the inclusion in the PT2C partition function for HCN of states that are not localized in the HCN well significantly affects the value of the PT2C rate constant at 4000 K, so this value should not be taken seriously.[7]

At low temperature, the transmission coefficients are sensitive to the extrapolation used to the product (HNC) minimum. In Table 4, we compare CVT/MEPSAG and CVT/CD-SCSAG rate constants calculated with two different values of the exponential range parameter, α, used to extrapolate from $s = 0.75$ bohr to the HNC minimum, as discussed in section 4. The results demonstrate that for room temperature and above, the transmission coefficients are not sensitive to the choice of α. However, $\alpha = 1.4$ bohr^{-1} produces a thinner adiabatic barrier than $\alpha = 1.1$ bohr^{-1} does, leading to transmission coefficients that are 50% (CVT/MEPSAG) and 74% (CVT/CD-SCSAG) higher at 200 K in both harmonic and anharmonic cases; at 250 K, the corresponding differences are 4% and 8%, respectively. (The CD-SCSAG rate constants are more sensitive to α because the effective reduced mass that accounts for reaction-coordinate curvature[11,56] is also modeled by an exponential extrapolation for $s > 0.75$ bohr.[2]) Thus, the anomalous local minimum in the MEP on the product side of the MCH PES that necessitates the use of an exponential extrapolation introduces some uncertainty in the rate constants that incorporate reaction-path tunneling, but only at very low temperatures.

6. Conclusions

In this work, we have presented a method for the calculation of anharmonic vibrational energy levels for the bound generalized normal modes along a reaction path that is based on second-order perturbation theory in curvilinear internal coordinates. Both asymmetric top and linear species have been considered, and the modifications needed when resonance occurs have been discussed; the details of these changes are given in the Supporting Information. For HCN, HNC, and the saddle point of the HCN/HNC isomerization reaction on the potential energy surface developed by Murrell, Carter, and Halonen,[36] this method yields an average absolute error in the zero point energy and fundamentals of only 2 cm^{-1}, compared to 63 cm^{-1} with the harmonic approximation. Canonical variational transition state theory (CVT) rate constants for the HCN/HNC isomerization reaction have been computed from generalized vibrational energy levels along the reaction path. We found that the results are not very sensitive to the choice of coordinates (curvilinear or Cartesian) for this system, but that, through a partial cancellation of errors, neglecting anharmonicity leads to rate constants that are about 4% larger at 298 K. We also demonstrated that simple perturbation theory (SPT)[34] leads to rate constants that are very close to those obtained by an explicit summation over vibrational energy levels except at very high temperature. This is quite encouraging because the direct summation over vibrational energy levels is impractical for systems of more than four atoms. Applications of this approach to other reactions of interest are currently underway in our laboratory.

Acknowledgment. I thank C. R. Quade and A. B. McCoy for several helpful discussions. The calculations reported here were carried out on the Miami University Department of Chemistry & Biochemistry's UNIX workstation, and the computer time is greatly appreciated.

Supporting Information Available: Equations S44−S74 give the modifications that are required in the perturbation theory anharmonicity coefficients and in the constant term, E_0, when $2\omega_i \approx \omega_j$ or $\omega_i + \omega_j \approx \omega_k$ resonances occur in asymmetric top and linear systems. This material is available free of charge via the Internet at http://pubs.acs.org.

References and Notes

(1) Truhlar, D. G.; Garrett, B. C. *Acc. Chem. Res.* **1980**, *13*, 440; Garrett, B. C.; Truhlar, D. G. *J. Chem. Phys.* **1979**, *70*, 1593; Garrett, B. C.; Truhlar, D. G. *J. Chem. Phys.* **1980**, *72*, 3460; Garrett, B. C.; Truhlar, D. G. *J. Phys. Chem.* **1979**, *83*, 1079; Garrett, B. C.; Truhlar, D. G. **1980**, *84*, 682; Garrett, B. C.; Truhlar, D. G. **1983**, *87*, 4553E; Garrett, B. C.; Truhlar, D. G. *J. Am. Chem. Soc.* **1979**, *101*, 5207; Garrett, B. C.; Truhlar, D. G. **1980**, *102*, 2559.

(2) Isaacson, A. D.; Truhlar, D. G. *J. Chem. Phys.* **1982**, *76*, 1380.

(3) Truhlar, D. G.; Isaacson, A. D.; Garrett, B. C. In *Theory of Chemical Reaction Dynamics*; Baer, M., Ed.; CRC Press: Boca Raton, FL, 1985; Vol. 4, pp 65−137.

(4) Truhlar, D. G.; Gordon, M. S. *Science* **1990**, *249*, 491.

(5) Isaacson, A. D.; Hung, S.-C. *J. Chem. Phys.* **1994**, *101*, 3928.

(6) Isaacson, A. D. *J. Chem. Phys.* **1997**, *107*, 3832.

(7) Isaacson, A. D. *J. Chem. Phys.* **2002**, *117*, 8778.

(8) Truhlar, D. G.; Kuppermann, A. *J. Am. Chem. Soc.* **1971**, *93*, 1840.

(9) Garrett, B. C.; Truhlar, D. G.; Grev, R. S.; Magnuson, A. W. *J. Phys. Chem.* **1980**, *84*, 1730; **1983**, *87*, 4554E.

(10) Garrett, B. C.; Truhlar, D. G. *J. Phys. Chem.* **1979**, *83*, 2921.

(11) Liu, Y.-P.; Lynch, G. C.; Truong, T. N.; Lu, D.-h.; Truhlar, D. G.; Garrett, B. C. *J. Am. Chem. Soc.* **1993**, *115*, 2408.

(12) Nathanson, G. A.; Garrett, B. C.; Truong, T. N.; Joseph, T.; Truhlar, D. G. *J. Chem. Phys.* **1991**, *94*, 7875.

(13) Jackels, C. F.; Gu, Z.; Truhlar, D. G. *J. Chem. Phys.* **1995**, *102*, 3188.

(14) Chuang, Y.-Y.; Truhlar, D. G. *J. Chem. Phys.* **1997**, *107*, 83; *J. Phys. Chem. A* **1998**, *102*, 242.

(15) Garrett, B. C.; Truhlar, D. G. *J. Chem. Phys.* **1979**, *70*, 1593.

(16) Miller, W. H.; Handy, N. C.; Adams, J. E. *J. Chem. Phys.* **1980**, *72*, 99.

(17) Morokuma, K.; Kato, S. In *Potential Energy Surfaces and Dynamics Calculations*; Truhlar, D. G., Ed.; Plenum: New York, 1981; pp 243−264.

(18) Miller, W. H. In *Potential Energy Surfaces and Dynamics Calculations*; Truhlar, D. G., Ed.; Plenum: New York, 1981; pp 265−286.

(19) Page, M. *Comput. Phys. Commun.* **1994**, *84*, 115.

(20) Tachibana, A.; Iwai, T. In *The Reaction Path in Chemistry: Current Approaches and Perspectives*; Heidrich, D., Ed.; Kluwer: Dordrecht, The Netherlands, 1995; pp 77−94.

(21) Isaacson, A. D. In *The Reaction Path in Chemistry: Current Approaches and Perspectives*; Heidrich, D., Ed.; Kluwer: Dordrecht, The Netherlands, 1995; pp 191−228.

(22) Nguyen, K. A.; Jackels, C. F.; Truhlar, D. G. *J. Chem. Phys.* **1996**, *104*, 6491.

(23) Garrett, B. C.; Truhlar, D. G. *J. Am. Chem. Soc.* **1979**, *101*, 4534; Garrett, B. C.; Truhlar, D. G. *J. Phys. Chem.* **1979**, *83*, 1915.

(24) Isaacson, A. D.; Truhlar, D. G.; Scanlon, K.; Overend, J. *J. Chem. Phys.* **1981**, *75*, 3017.

(25) Isaacson, A. D.; Truhlar, D. G. *J. Chem. Phys.* **1981**, *75*, 4090; Isaacson, A. D.; Truhlar, D. G. *J. Chem. Phys.* **1984**, *80*, 2888.
(26) Isaacson, A. D.; Zhang, X.-G. *Theor. Chim. Acta* **1988**, *74*, 493.
(27) Zhang, Q.; Day, P. N.; Truhlar, D. G. *J. Chem. Phys.* **1993**, *98*, 4948.
(28) Quade, C. R. *J. Chem. Phys.* **1976**, *64*, 2783.
(29) McCoy, A. B.; Sibert, E. L. *J. Chem. Phys.* **1990**, *92*, 1893.
(30) McCoy, A. B.; Sibert, E. L. *J. Chem. Phys.* **1991**, *95*, 3476.
(31) McCoy, A. B.; Sibert, E. L. In *Advances in Molecular Vibrations and Collision Dynamics*; JAI Press: Greenwich, CT, 1991; Vol. 1A, pp 255−282.
(32) McCoy, A. B.; Sibert, E. L. *J. Chem. Phys.* **1991**, *95*, 7449.
(33) Truhlar, D. G.; Olsen, R. W.; Jeannotte, A. C.; Overend, J. *J. Am. Chem. Soc.* **1976**, *98*, 2373; Carney, G. D.; Sprandel, L. L.; Kern, C. W. *Adv. Chem. Phys.* **1978**, *37*, 305.
(34) Truhlar, D. G.; Isaacson, A. D. *J. Chem. Phys.* **1991**, *94*, 357.
(35) Isaacson, A. D. *J. Chem. Phys.* **1998**, *108*, 9978.
(36) Murrell, J. N.; Carter, S.; Halonen, L. O. *J. Mol. Spectrosc.* **1982**, *93*, 307.
(37) Gazdy, B.; Bowman, J. M. *J. Chem. Phys.* **1991**, *95*, 6309.
(38) Yang, X.; Rogaski, C. A.; Wodtke, A. M. *J. Opt. Soc. Am. B* **1990**, *7*, 1835.
(39) Wilson, E. B., Jr.; Decius, J. C.; Cross, P. C. *Molecular Vibrations*; McGraw-Hill: New York, 1955.
(40) In the spectroscopists units of ref 28, Q_i has units of $cm^{1/2}$, $P_i = -i\partial/\partial Q_i$ has units of $cm^{-1/2}$, and H, V, and V' have units of cm^{-1}.
(41) Many of the basic matrix elements needed here can be obtained from Appendix III of ref 39 by replacing γ by ω and by dividing P by $\hbar$. In addition, note that the Hamiltonian must be properly Hermitianized.[28]
(42) Hameka, H. F. *Quantum Mechanics*; Wiley: New York, 1981.
(43) Nielsen, H. H. *Phys. Rev.* **1950**, *77*, 130.
(44) Shaffer, W. H. *Rev. Mod. Phys.* **1944**, *16*, 245.
(45) Nielsen, H. H. *Rev. Mod. Phys.* **1951**, *23*, 90.
(46) Barchewitz, M. P. *Spectroscopie Infrarouge*; Gauthier-Villars: Paris, 1961.
(47) In $x_{l_s l_s}$, a contribution arising from the $A^{zz}{}_{\theta\theta\theta}$ term in $H^{(2)}$ has been omitted; it is expected to be quite small.
(48) Sibert, E. L. *J. Chem. Phys.* **1989**, *90*, 2672.
(49) Nielsen, H. H. *Encl. Phys.* **1959**, *37*, 173.
(50) Califano, S. *Vibrational States*; Wiley: London, 1976.
(51) Nakagawa, T.; Morino, Y. *J. Mol. Spectrosc.* **1968**, *26*, 496; Nakagawa, T.; Morino, Y. *Bull. Chem. Soc. Jpn.* **1969**, *42*, 2212.
(52) Harding, L. B.; Ermler, W. C. *J. Comput. Chem.* **1985**, *6*, 13; Ermler, W. C.; Hsieh, H. C.; Harding, L. B. *Comput. Phys. Commun.* **1988**, *51*, 257.
(53) Tennyson, J.; Henderson, J. R.; Fulton, N. G. *Comput. Phys. Commun.* **1995**, *86*, 175; Tennyson, J.; Sutcliffe, B. T. *Mol. Phys.* **1986**, *58*, 1067.
(54) Romanowski, H.; Bowman, J. M. POLYMODE, Quantum Chemistry Program Exchange program 496, *QCPE Bull.* **1985**, *5*, 64; Romanowski, H.; Bowman, J. M.; Harding, L. B. *J. Chem. Phys.* **1985**, *82*, 4155.
(55) Schwarz, H. R. *Numerical Analysis*; Wiley: Chichester, U.K., 1989.
(56) Lu, D.-h.; Truong, T. N.; Melissas, V. S.; Lynch, G. C.; Liu, Y.-P.; Garrett, B. C.; Steckler, R.; Isaacson, A. D.; Rai, S. N.; Hancock, G. C.; Lauderdale, J. C.; Joseph, T.; Truhlar, D. G. *Comput. Phys. Commun.* **1992**, *71*, 235; Steckler, R.; Hu, W.-P.; Liu, Y.-P.; Lynch, G. C.; Garrett, B. C.; Isaacson, A. D.; Melissas, V. S.; Lu, D.-h.; Truong, T. N.; Rai, S. N.; Hancock, G. C.; Lauderdale, J. G.; Joseph, T.; Truhlar, D. G. *Comput. Phys. Commun.* **1995**, *88*, 341.
(57) Marcus, R. A. *J. Chem. Phys.* **1966**, *45*, 4493; Marcus, R. A. **1969**, *49*, 2617.
(58) Skodje, R. T.; Truhlar, D. G.; Garrett, B. C. *J. Chem. Phys.* **1982**, *77*, 5955.